Transpirational heat and momentum transfer from a rotating cylinder
by Robert John Spannuth

A thesis submitted to the Graduate Faculty in partial fulfillment of the requirements for the degree of DOCTOR OF PHILOSOPHY in Chemical Engineering
Montana State University

Abstract:
In this investigation, heat transfer and moment coefficients were determined with and without transpiration mass transfer for a rotating cylinder in a finite medium with turbulent flow. Reynolds numbers ranged from 27,000 to 330,000. Mass transfer rates expressed as the ratio (Formula not captured by OCR) ranged from 250 to 35,000.

For the case of no mass transfer, moment coefficients were in excellent agreement with published data; however, there is no published data for heat transfer coefficients in the range of Reynolds numbers used in this experiment. In the moment coefficient experiment an apparent flow transition was observed at a Reynolds number of 55,000.

With transpiration, heat transfer and moment coefficients increased . with mass transfer. This phenomenon is consistent with the hypothesis that a laminar sublayer does not exist on the surface of a rotating cylinder for turbulent flow. The most significant result of this investigation is that the heat transfer coefficients increased much more dramatically with Injection than did the moment coefficients.

TRANSPIRATIONAL HEAT AND MOMENTUM TRANSFER FROM A ROTATING CYLINDER

by

ROBERT JOHN SPANNUTH

A thesis submitted to the Graduate Faculty in partial fulfillment of the requirements for the degree

of

DOCTOR OF PHILOSOPHY

in

Chemical Engineering

Approved:

Head, Major Department

Chairman, Examining Committee

Graduate Dean

MONTANA STATE UNIVERSITY
Bozeman, Montana

March, 1974

ACKNOWLEDGMENT

The author is grateful to the National Science Foundation for a three-year fellowship to help support his family through graduate school and for a grant to purchase equipment for this project. Special thanks go to Silas Huso and James Tillery, technicians for the Chemical Engineering Department, and Gordon Williamson, technician for the Mechanical Engineering Department, for their efforts in building the experimental equipment, and to the author's advisor, Dr. William E. Genetti, for his direction of the project. Finally, the author is appreciative of the sacrifices of his family and the moral support of his fishing partners, chess mates, and basketball teammates.

TABLE OF CONTENTS

LIST OF TABLES

LIST OF FIGURES

ABSTRACT

In this investigation, heat transfer and moment coefficients were determined with and without transpiration mass transfer for a rotating cylinder in a finite medium with turbulent flow. Reynolds numbers ranged from 27,000 to 330,000. Mass transfer rates expressed as the ratio V_{θ_o}/V_{r_o} ranged from 250 to 35,000.

For the case of no mass transfer, moment coefficients were in excellent agreement with published data; however, there is no published data for heat transfer coefficients in the range of Reynolds numbers used in this experiment. In the moment coefficient experiment an apparent flow transition was observed at a Reynolds number of 55,000. With transpiration, heat transfer and moment coefficients increased with mass transfer. This phenomenon is consistent with the hypothesis that a laminar sublayer does not exist on the surface of a rotating cylinder for turbulent flow. The most significant result of this investigation is that the heat transfer coefficients increased much more dramatically with injection than did the moment coefficients.

I. INTRODUCTION

Transpiration from a surface, that is, the existence of a velocity normal to the surface due to mass transfer, occurs in heterogeneous catalysis, combustion and evaporation at low pressures or near the boiling point. Other examples of transpiration include cooling of aerodynamic surfaces in high speed flights, cooling of turbine blades, and cooling of rocket nozzles. The objective of this investigation was the study of transpiration from a rotating cylinder in a finite medium with possible application in the cooling of shafts. Other applications may include the use of a rotating cylinder as a blender, spray applicator, or chemical reactor.

Early research on transpiration dealt with flat plates. Pioneer papers include the theoretical studies of Rubesin (1) and Dorrance and Dore (2) and the experimental work of Mickley _et al_. (3) in the 1950's. Since 1960 many contributions have been made with a major contributor being W. M. Kays (4). Mass transfer from a flat plate is discussed in Bird, Stewart, and Lightfoot (5). By comparison there are relatively few investigations of transpiration with geometries other than flat plates. Elzy and Wicks (6) and Johnson and Hartnett (7) have studied mass transfer from a stationary cylinder in crossflow. Cozart (8) has investigated transpiration from a rotating disc. Erickson _et al_. (9) have studied theoretically mass transfer from a moving, continuous flat plate. Krishan and Rai (10) and Mishra (11) have studied theoretically temperature and velocity profiles, respectively, for transpiration between two concentric cylinders for viscous flow. Bahl (12) has studied the stability of viscous flow between concentric cylinders with transpiration. With the exception of flat plates, there is little data regarding transpiration from other geometries, particularly cylinders. Thus, the purpose of this investigation was the determination of the effect of mass transfer on the heat transfer coefficients and moment coefficients for a rotating cylinder in a finite medium.

Although the principal concern of this investigation was the effect of transpiration on heat and momentum transfer, heat transfer coefficients and moment coefficients for a rotating cylinder with no mass transfer were also determined. A significant amount of work on heat and momentum transfer without mass transfer for concentric cylinders has been done. A representative list of contributors for heat transfer between concentric cylinders includes Gazley (13), Becker and Kaye (14), Björklund and Kays (15), and Sharman *et al.* (16). A paper on moment coefficients for rotating cylinders by Bilgen and Boulos (17) summarizes the work of Taylor (18), Wendt (19), Donnelly (20), and Theodorsen and Regier (21). Finally, a great volume of work has been done on stability of flow between rotating concentric cylinders with Taylor (22) and Chandrasekhar (23) being important contributors.

II. RESEARCH OBJECTIVES

The purpose of this investigation was to study the effect of mass transfer on heat and momentum transfer from a rotating cylinder in a finite medium. Heat transfer coefficients and moment coefficients were determined for a rotating, porous cylinder by varying mass injection rates and angular velocities. The experiment consisted of rotating a porous cylinder in a tank filled with the same fluid as the injection fluid and measuring temperature differences across the cylinder wall and across the tank to determine the heat transfer coefficient. To determine the moment coefficient, the torque on the rotating cylinder was measured.

A heat balance for the cylinder and tank system includes the following terms: heat transfer due to molecular action across the tank (q_m), heat transfer due to bulk motion inside the cylinder (q_i), and heat transfer due to bulk motion at the wall of the cylinder (q_w). Although some axial heat transfer might be expected due to natural convection, it was considered to be negligible with respect to radial heat transfer. Indeed, Chandrasekhar (24) and Dropkin and Globe (25) have shown that rotation greatly reduces natural convection even when an axial temperature gradient is imposed. Of course, there was no angular heat transfer. Finally, heat transfer due to radiation was neglected because of the high absorptivity of water. [Heat transfer due to radiation is given by

$$q_r = \frac{\sigma\,(T_c^{\,4} - T_w^{\,4})}{\dfrac{1-\varepsilon_c}{\varepsilon_c A} + \dfrac{1-\varepsilon_w}{\varepsilon_w A} + \dfrac{1}{AF_{cw}}}, \tag{1}$$

where the system under consideration is the cylinder denoted by the subscript c and the layer of water next to the cylinder denoted by the subscript w. Clearly, the areas are the same and the view factor F_{cw} is one. For ε_w approximately equal to one,

$$q_r = \varepsilon_c A\sigma(T_c^{\,4} - T_w^{\,4}). \tag{2}$$

But the difference between T_c and T_w is very small so q_r is negligible].

The heat transfer terms were defined as follows:

$$q_m = \mathring{h}A(T_c - T_t), \tag{3}$$

$$q_i = mC_p(T_i - T_{ref}), \tag{4}$$

and

$$q_w = mC_p(T_c - T_{ref}). \tag{5}$$

Clearly,

$$q_i - q_w = mC_p(T_i - T_c) \tag{6}$$

gives the heat transfer across the cylinder wall. Equating the expressions for heat transfer across the cylinder wall and heat transfer across the tank results in the defining equation for the heat transfer coefficient with mass transfer, i.e.,

$$\mathring{h} = mC_p(T_i - T_c)/A(T_c - T_t). \tag{7}$$

The heat transfer coefficient with no mass transfer—h—was determined by extrapolating a plot of h versus m to m = 0.

To determine the moment coefficient, the torque on the rotating cylinder was measured. From Schlichting (26), the moment coefficient was defined by the equation,

$$C_m = \frac{\tau g_c}{0.5\ \pi \rho \omega^2 R_c^4 L} \quad (8)$$

III. EQUIPMENT

A. HEAT TRANSFER COEFFICIENTS

Basically, the heat transfer experiment consisted of rotating a porous cylinder in a tank. The heat source was the injection fluid; a refrigerated cooling bath served as the heat sink. Figure 1 shows the method of fixing the porous cylinders to a rotating shaft with collars. Two porous cylinders--1-1/2 inches I.D. by 1-31/32 inches O.D. by 5-3/4 inches long and 2-1/4 inches I.D. by 2-3/4 inches O.D. by 5-3/4 inches long--were placed concentrically around the shaft. Allen screws perpendicular to the shaft secured the bottom collar to the shaft. The top collar was screwed into tubes connected to the bottom collar compressing the porous cylinders into O-ring gaskets. Leakage between the shaft and collars was prevented by stop-cock grease. The inner cylinder was used to diffuse the flow and assure more uniform flow through the outer cylinder. Due to the problem of corrosion, the shaft was stainless steel, the porous cylinders were sintered bronze purchased from Thermet, and the collars were aluminum. The most difficult aspect of the heat transfer experiment involved the installation of the thermocouples in the porous cylinders. Because of the very small clearances, a fine, supple thermocouple wire was required. Thus, the chromel-alumel thermocouple wire chosen was 30 gauge with no waterproof coating, since a waterproof coating would stiffen the wire too much in addition to increasing the diameter significantly. To protect the wire from water and subsequent shorting, the thermocouple wire outside the shaft was placed inside a 1/16 inch O.D. stainless steel tube. Epoxy glue was used to seal the

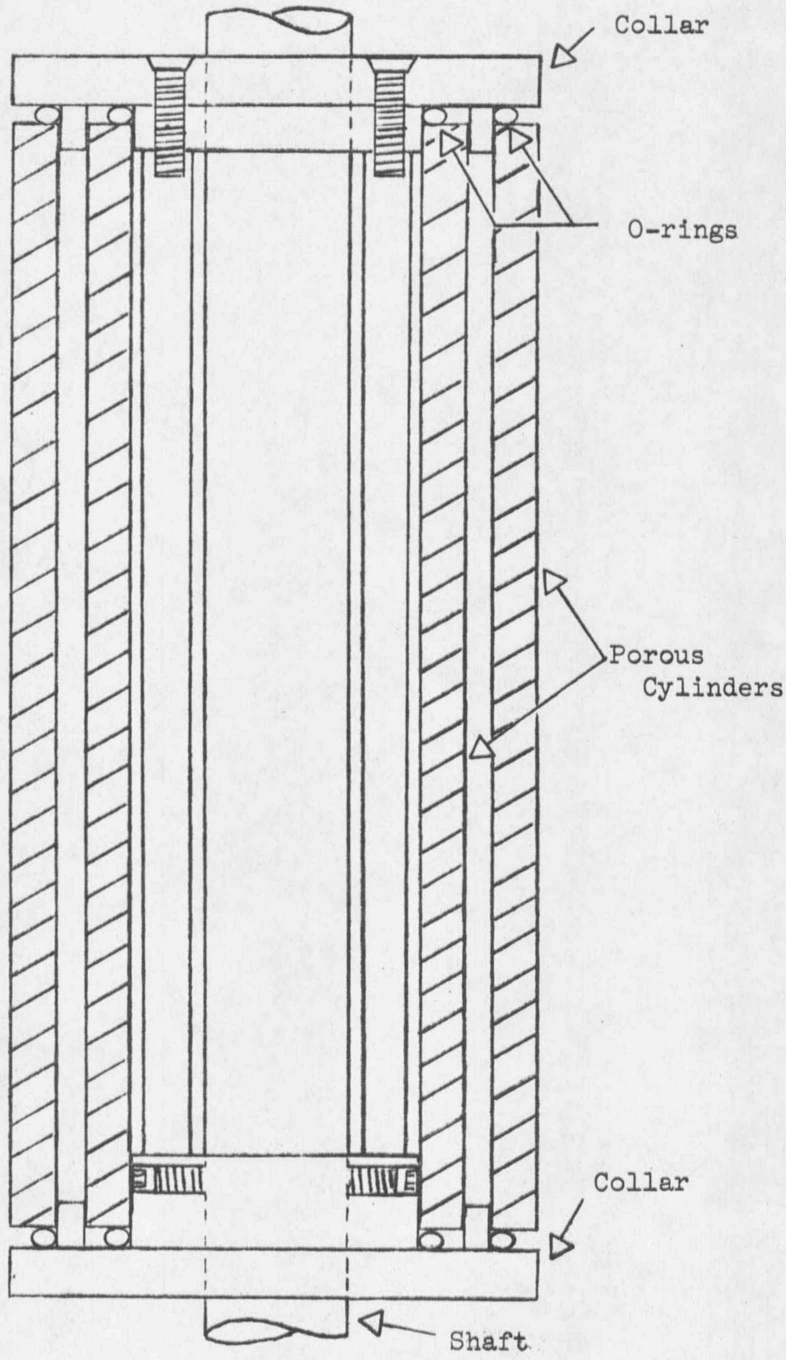

Figure 1. Porous Cylinders and Collars

thermocouple junctions to the tubes and the tubes to the shaft (see Figure 2). To transfer the emf signals from the rotating shaft a Power Instruments, Inc. model No. 6118-111-4 slip ring was used (see Figure 3). Above rotation speeds of 100 RPM there was no noise in the slip ring; occasionally below 100 RPM, a satisfactory reading could be obtained only by stopping rotation. EMF was measured on an extremely accurate potentiometer; readings could be made in millivolts to four decimals--an accuracy probably not inherent in the thermocouples.

The porous cylinder was rotated in an 11-3/4 inches diameter by 7-1/4 inches high aluminum tank with phenolic-resin board stiffening rings at top and bottom. Brass bolts were used to secure the stiffening rings. The cooling bath around the tank was made from 1/4 inch lucite and had the dimensions 16 inches by 16 inches by 10 inches high. The cooling fluid was water; overflow from the tank due to injection entered the cooling bath; an overflow weir on the cooling bath maintained constant level. The same wire was used for the tank wall thermocouple as for the cylinder thermocouples. The portion of the thermocouple wire in the cooling bath was waterproofed by slipping a length of plastic tube over it and sealing with a silicone glue at the tank wall.

The distilled water used for injection was filtered and heated and entered the shaft by means of a rotating union. Flow rates were determined using calibrated rotameters. The filter consisted of a 2 inch diameter porous plate covered by 0.8 micron filter paper. A sufficient

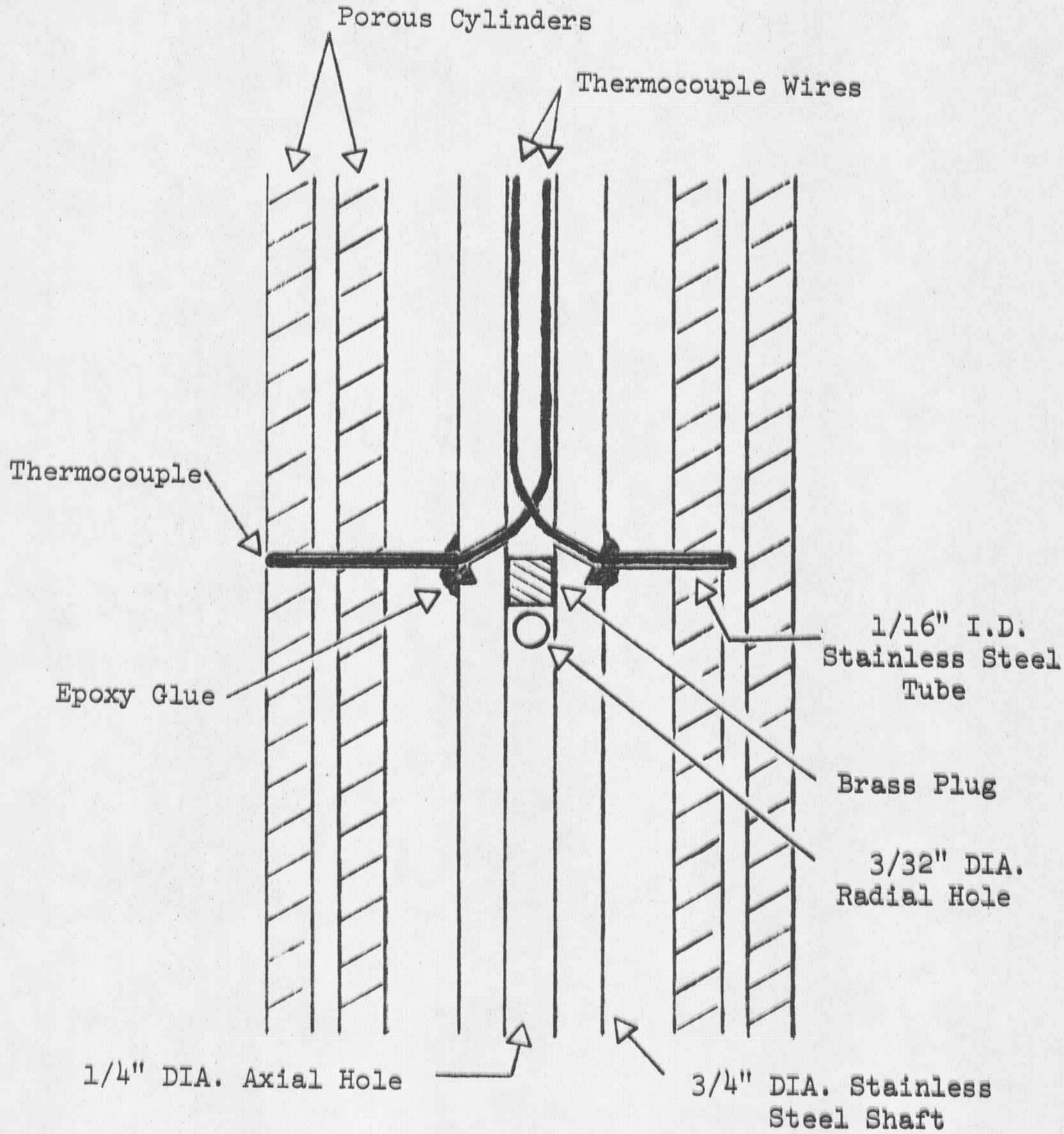

Figure 2. Thermocouple Location

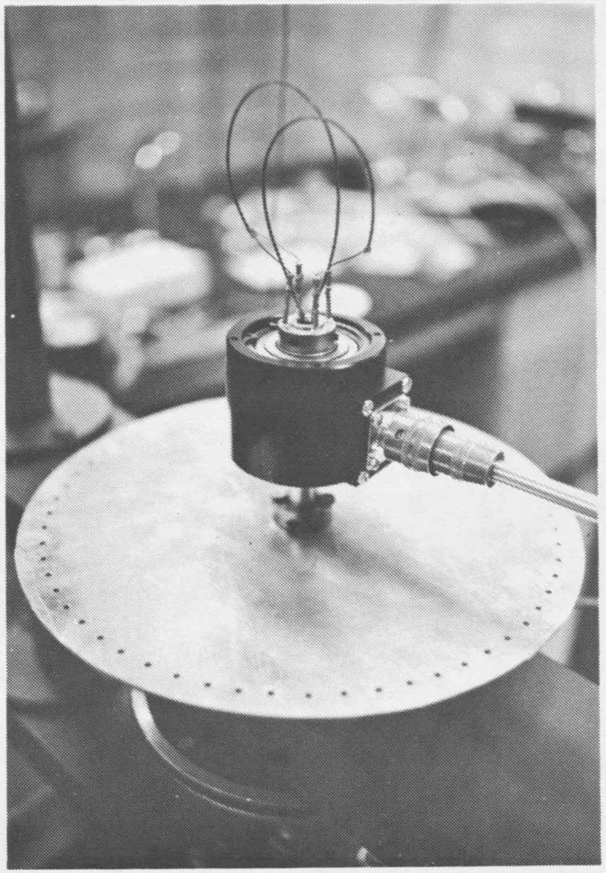

Figure 3. Slip Ring

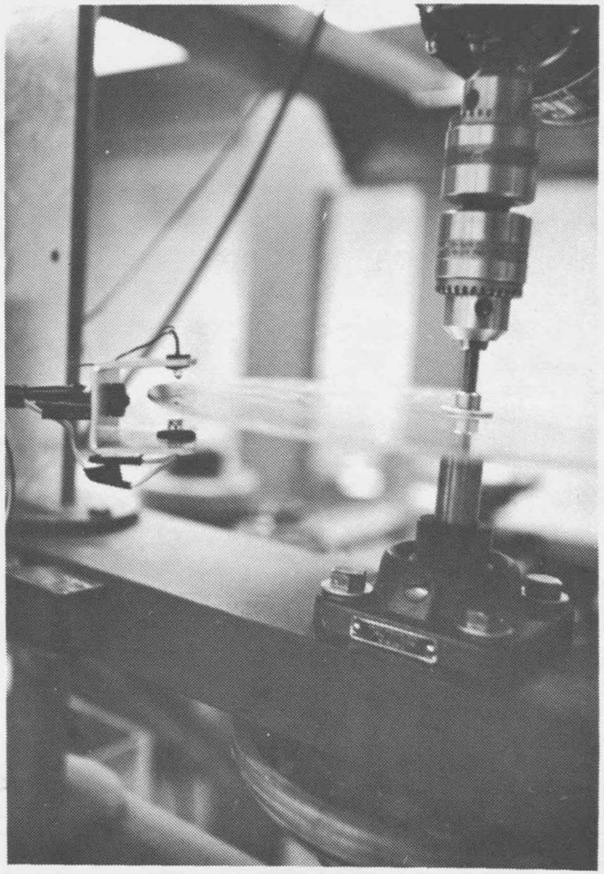

Figure 4. Light Source, Photocell, and Disk

amount of scale was present in the distilled water system to necessitate changing of the filter one or more times during an operating day, depending on flow rates. The heater was a 1 inch diameter by 36 inches long pyrex tube wrapped with 25 feet of nichrome wire. The heating rate was controlled by a rheostat and outlet temperatures were limited to less than 150°F. due to localized boiling in the tube. The rotating union was purchased from Deublin Company. All equipment not purchased for this project was available within the Chemical Engineering department or fabricated by technicians from the Chemical Engineering or Mechanical Engineering departments at Montana State University.

Heat removal in the cooling bath was accomplished by means of cooling coils and a refrigeration unit. A small pump was used to circulate the cooling bath in order to prevent freezing on the coils. The refrigeration unit (from an old refrigerator) had a rather small duty--approximately 1000 BTU/hr--so that at high injection rates the bath temperature reached 15°C. On the other hand, at very low flow rates, warm water was added to the cooling bath to prevent freezing.

The rotating shaft was held in place by three sets of flange bearings. Leakage around the shaft at the bottom of the tank was eliminated by a screw-type packing gland. The shaft was rotated by a 1/2 HP, 1725 RPM motor with a pulley on the motor, an idler pulley, and a pulley on the shaft so that several speeds were available.

Finally the rotational speed in RPM's was determined using a light

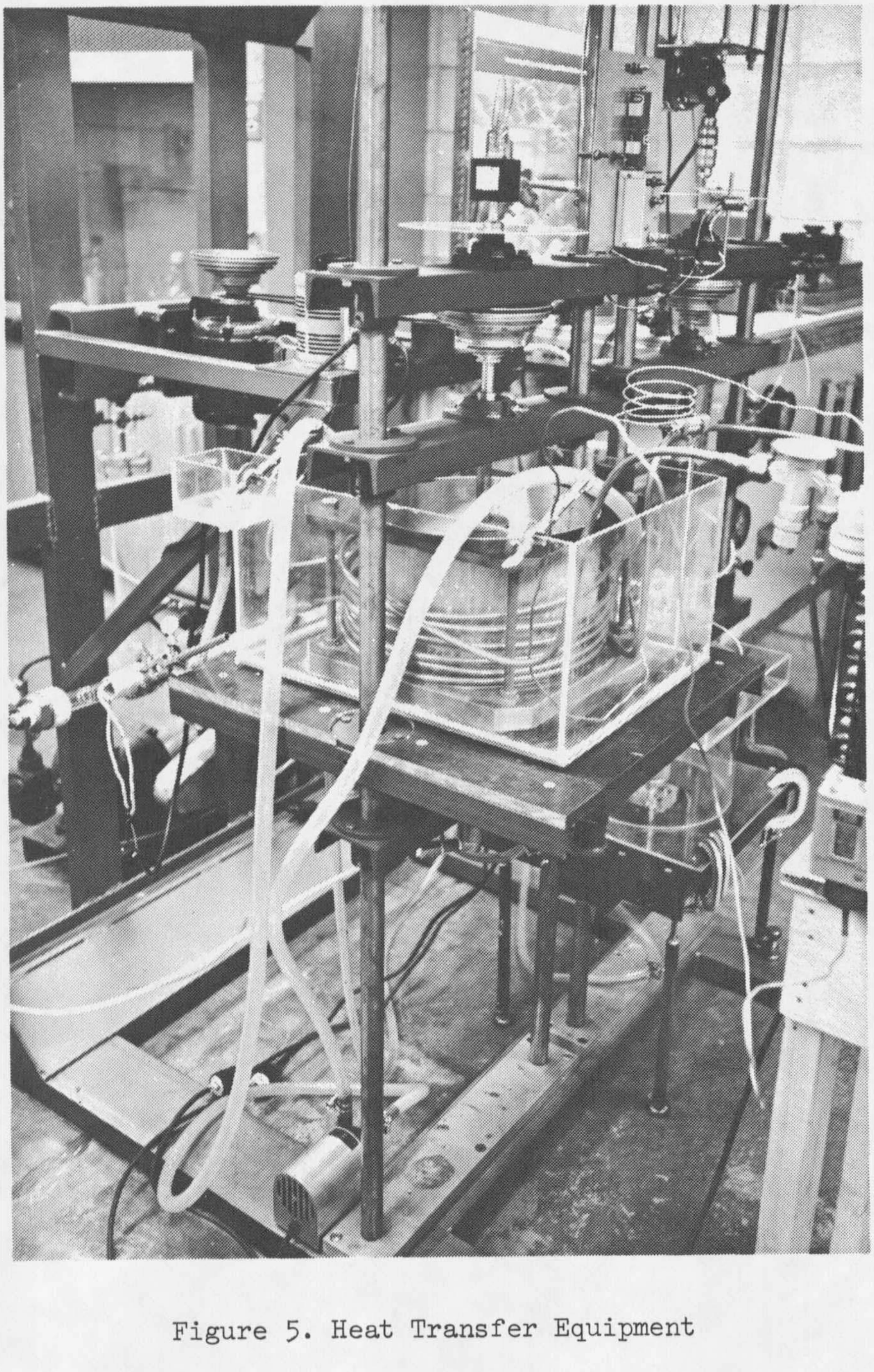

Figure 5. Heat Transfer Equipment

source and photocell, a disk with 60 evenly spaced holes, and a Berkeley eput meter (see Figure 4). Because the eput meter counted for only one second, the 60-hole disk gave RPM as follows:

$$\text{RPM} = \frac{\text{rev}}{\text{min}} = \frac{\text{counts}}{\text{sec}} \times \frac{\text{rev}}{60\text{ sec.}} \times \frac{60\text{ sec.}}{\text{min.}}$$

Figure 5 is an overall view of the heat transfer equipment.

During experimental runs "equilibrium" was usually reached after two hours, so that in the next hour millivolt readings would change only in the third decimal and the heat transfer coefficient would vary by usually not more than 2%.

B. MOMENT COEFFICIENTS

Although the experiments for determining heat transfer coefficients and moment coefficients were analagous, the equipment for the moment coefficient determinations was much more sophisticated. To measure torque on the rotating cylinder, other sources of torque in the equipment were eliminated or made relatively small. For example, the commercially available rotating union with the smallest torque required 64 oz-in. Since the largest torque measured in the experiment was 0.68 oz-in, this rotating union was clearly unacceptable. Similarly, conventional bearings and packing glands require extremely large torques. Thus, "frictionless" bearings, packing gland, and rotating union were needed.

Virtually frictionless air bearings were purchased from Professional Instruments Company. However, with no low-torque rotating unions commercially available, the feasibility of the experiment was not assured until this investigator developed the "frictionless rotating union." Thus, the importance of the "frictionless rotating union" to the experiment cannot be overestimated, however simple the device may appear.

Actually, "frictionless rotating union" is a misnomer since the device was stationary; rather, the device was a frictionless substitute for a rotating union. A description of the "frictionless rotating union" follows (see Figures 6 and 7).

The device, constructed of lucite, consisted of six sections--four of which had the dimensions 3 inches by 3 inches by 1/2 inch with a 2 inch diameter by 1/4 inch machined groove, the fifth had the dimensions 3 inches by 3 inches by 1 inch with a 1-1/2 inch diameter by 3/4 inch machined groove, and the sixth had the dimensions 3 inches by 3 inches by 1/4 inch and was used as a spacer above the largest section. The six sections were pinned together and the shaft hole drilled. The outside two sections, containing the "air chambers," had 1/8 inch fittings for compressed air. The next sections from the outside, containing the "leak chambers," were connected by a small hole with an 1/8 inch fitting in the bottom section open to the atmosphere. The largest section, containing the "injection chamber," had a 1/4 inch fitting for the injection fluid and an 1/8 inch fitting open to the atmosphere.

Figure 8 is a diagram of the equipment location for the moment coefficient experiment. By connecting a drive shaft to the shaft holding the porous cylinder with a torquemeter, the torque on the shaft, predomi-

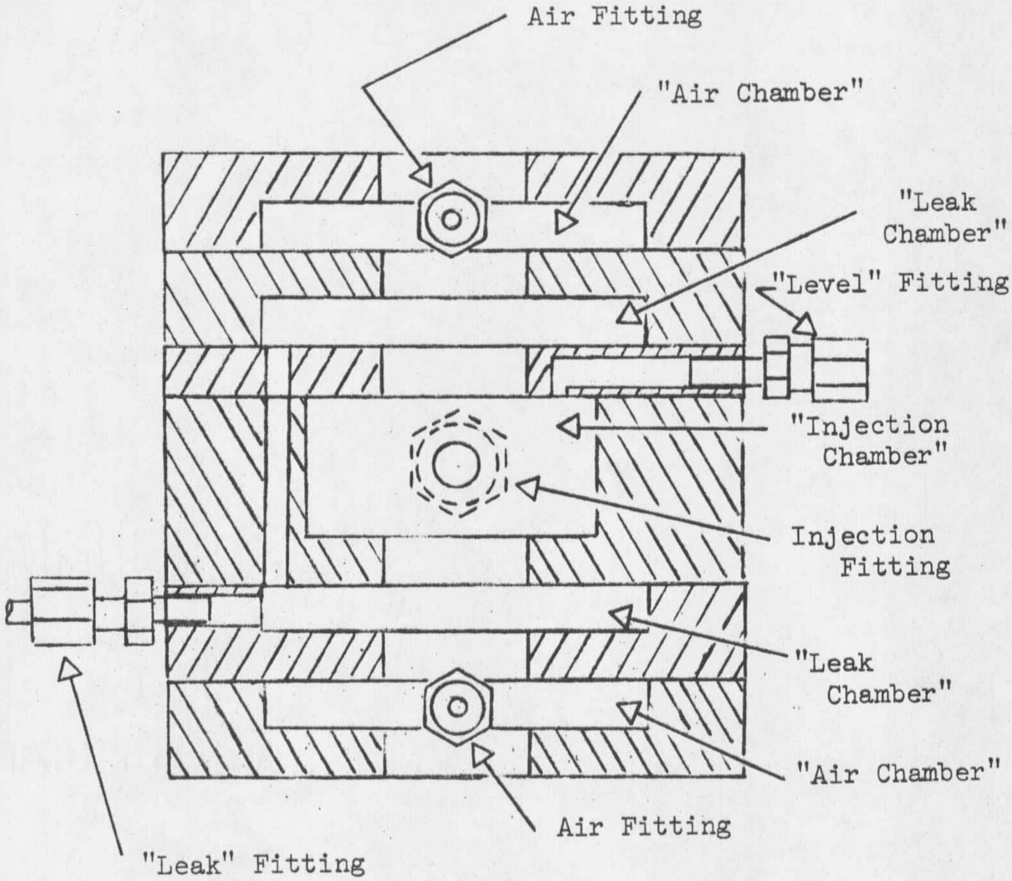

Figure 6. "Frictionless Rotating Union"

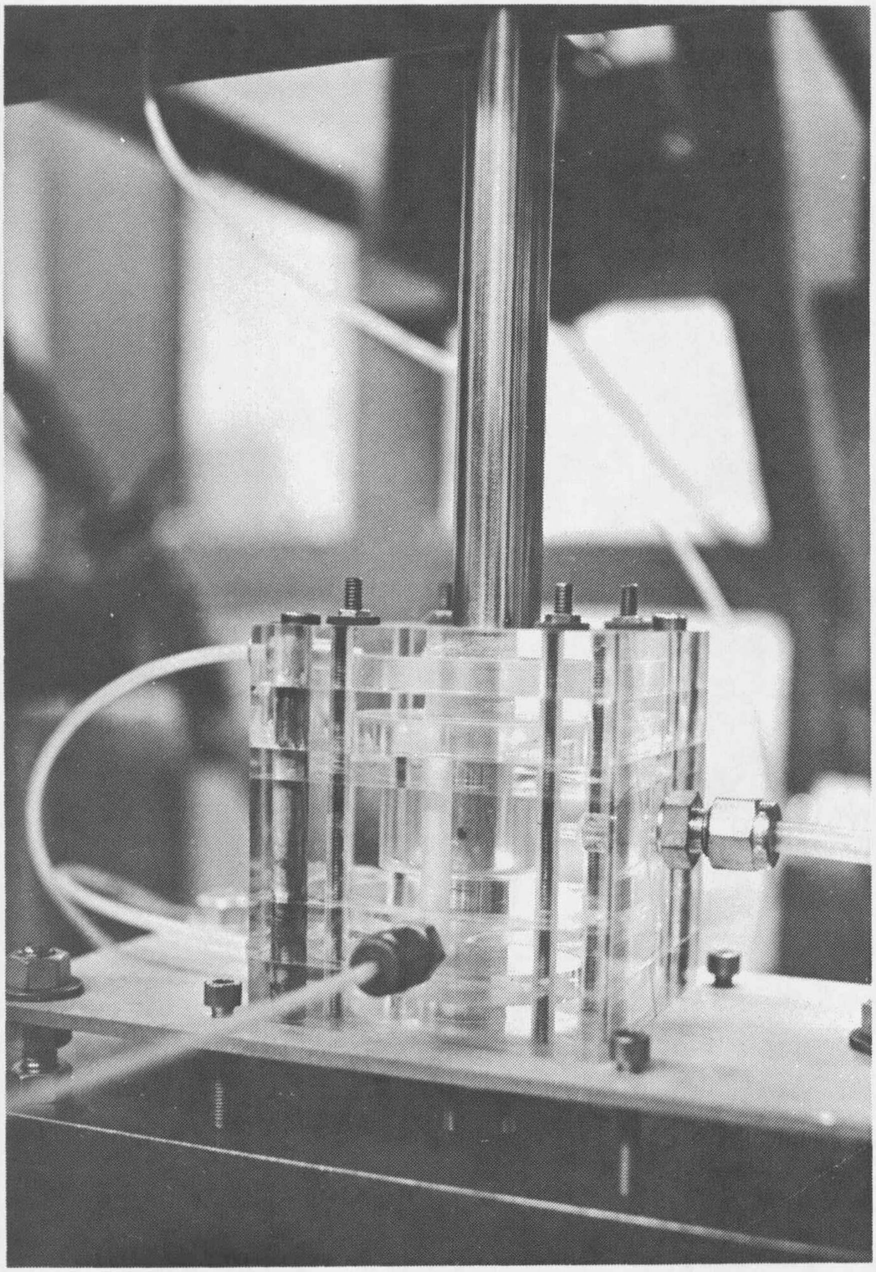

Figure 7. "Frictionless Rotating Union"

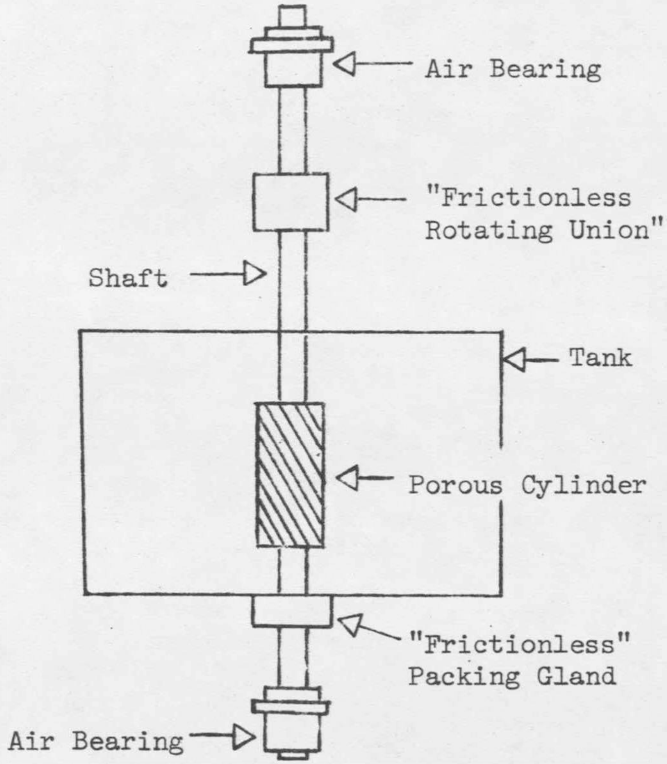

Figure 8. "Frictionless" Shaft

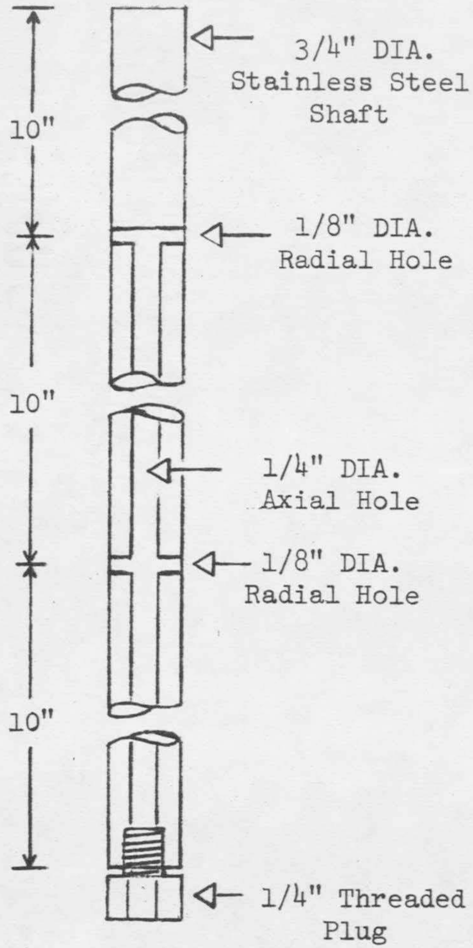

Figure 9. Moment Coefficient Experiment Shaft

nantly due to the porous cylinder, could be determined as a function of angular speed and injection. The machined shaft purchased from Twentieth Century Machine Company is shown in Figure 9.

From Figure 9, it can be seen that fluid was injected radially into the shaft, where it flowed axially down the shaft and then radially again into the porous cylinder. Thus, the top radial holes in the shaft were aligned in the center of the "injection chamber" of the "frictionless rotating union." As fluid was pumped into the "injection chamber," the compressed air flow into the "air chambers" was adjusted so that all the fluid flow was forced into the shaft through the radial holes. Although the "frictionless rotating union" could be operated so that no fluid leaked from the "injection chamber," in general some leakage was allowed so that there was no chance of air entering the "injection chamber" with the result of air's being injected through the porous cylinder. The amount of fluid entering the "leak chambers" was actually very small. Finally, the level of fluid in the "injection chamber" was adjusted by means of the 1/8 inch fitting. (See appendix for more information regarding operation of the "frictionless rotating union."). The "frictionless packing gland" was built on the same principle as the "frictionless rotating union." That is, the packing gland consisted of an "air chamber" for compressed air and a "leak chamber" for leakage.

Although the equipment was assembled on a very carefully machined, stable set of platforms, alignment was troublesome due to the very small tolerances--0.002 inch--between the shaft and the rotating union and packing gland. Use of leveling screws facilitated alignment, however. Because the air bearings were attached to the shaft by means of O-rings, the air bearings were essentially self-aligning. Since the residual torque, i.e., the torque produced in an empty tank with no injection, varied from 0.02 oz-in at 30 RPM to 0.063 oz-in at 360 RPM, the equipment was indeed virtually frictionless. The torque used in the moment coefficient calculations was the torque measured with a full tank less the residual torque.

Finally, to determine whether or not changes in torque during injection could be attributed to the "frictionless rotating union" rather than to injection through the porous cylinder, the plug on the bottom of the shaft was removed and injection was made directly down the shaft and out. No flow was observed from the porous cylinder; furthermore, the residual torque was unchanged even at the highest injection rate used in the experiment. Therefore, it was concluded that the "frictionless rotating union" was indeed frictionless.

The tank used in the moment coefficient experiments was lucite with the dimensions 11-1/2 inches diameter by 10 inches high. Overflow from the tank was caught in an overflow weir and recycled to the feed tank. The porous cylinders and collars were identical to those used in the heat transfer experiments. However, a slight eccentricity in the porous cylinders produced some difficulty with alignment at rotational speeds above 100 RPM.

Distilled water from the feed tank was pumped by a small capacity worm wheel pump through a filter and a calibrated rotameter to the "frictionless rotating union." A surge tank was installed after the pump to eliminate flow pulsation due to the nature of the pump. Because of persistent scale in the pump a larger filter--a 4 inch porous stainless steel plate with 0.8 micron filter paper--was required for the moment coefficient experiment than for the heat transfer experiment and it had to be changed more frequently. Fortunately, runs in the moment coefficient experiment could be made in a matter of minutes. A pump was required for the moment coefficient experiment since the "frictionless rotating union" did not operate well below 20 psi and the maximum pressure on the distilled water system was 13 psi. Below 20 psi, which included the pressure drop through the filter, air entered the "injection chamber" from the lower "leak chamber" even with no air pressure on the lower "air chamber" of the "frictionless rotating union." Probably a reason for this phenomenon could have been found and a solution determined, but increasing pressure above 20 psi was more expedient, particularly since the pump was already installed because the pressure drops through both the heat transfer and moment coefficient experiments were expected to be much higher than actually found.

Two Power Instruments, Inc. torquemeters were used to determine the torque on the shaft--Model No. 781-B-10 in the range of 0.5 to 10.0 gm-cm and Model No. 783-C-1 in the range of 0.05 to 1.0 oz-in (see Figure 10). A flexible aluminum coupling was used to attach the torquemeter to the shaft with the porous cylinder to facilitate alignment. It was estimated that approximately 5% of the torque readings could be attributed to the shaft and collars and the remainder to the porous cylinder; therefore, this error was ignored and the torquemeter readings were used directly in determining moment coefficients. In practice no torque was observed for the shaft and collars. Because the torquemeter was attached directly to the shaft and rotated with the shaft, a Strobotac strobe light was used to read the torquemeter.

Although it was intended to use the same motor and pulley arrangement to drive the moment coefficient experiment as was used in the

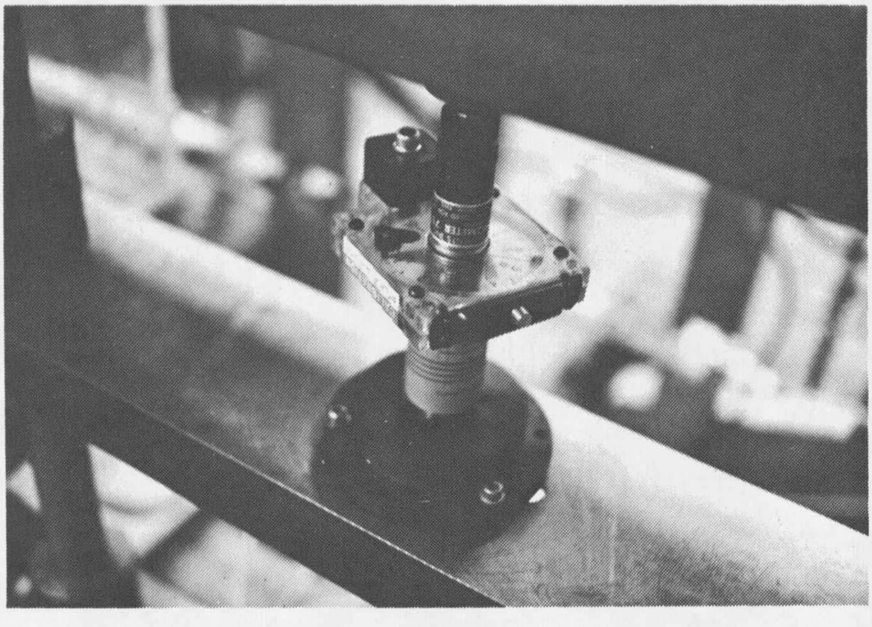

Figure 10. Torquemeter

heat transfer experiment, enough vibration resulted to affect alignment of the shaft. Furthermore, the synchronous motor could not be started slow enough with a rheostat to prevent overload on the gm-cm torquemeter when overcoming the inertia of the shaft. Therefore, a small brush motor was installed directly in line with the shaft. Because the brush motor had a low torque--4.7 in-lb--resistance in the flange bearings aligning the drive shaft resulted in variations in the rotational speed. To overcome these speed variations, the pulley system was connected with the synchronous motor turned off, thereby creating a flywheel effect. Finally, the rotational speed in the moment coefficient experiment was determined in the same manner as in the heat transfer experiment.

Figure 11 is a diagram of the air system for the moment coefficient experiment. Although not previously mentioned, the air bearings required clean, dry air at 100 psi. A large filter containing Dry-rite as well as a porous stainless steel plate and 0.8 micron filter paper was installed in the main air supply line. In addition, Gelman filters were placed on the individual supply lines to the air bearings (two per air bearing).

Figure 12 is an overall view of the moment coefficient equipment Figures 13 and 14 are overall view of the entire experimental equipment.

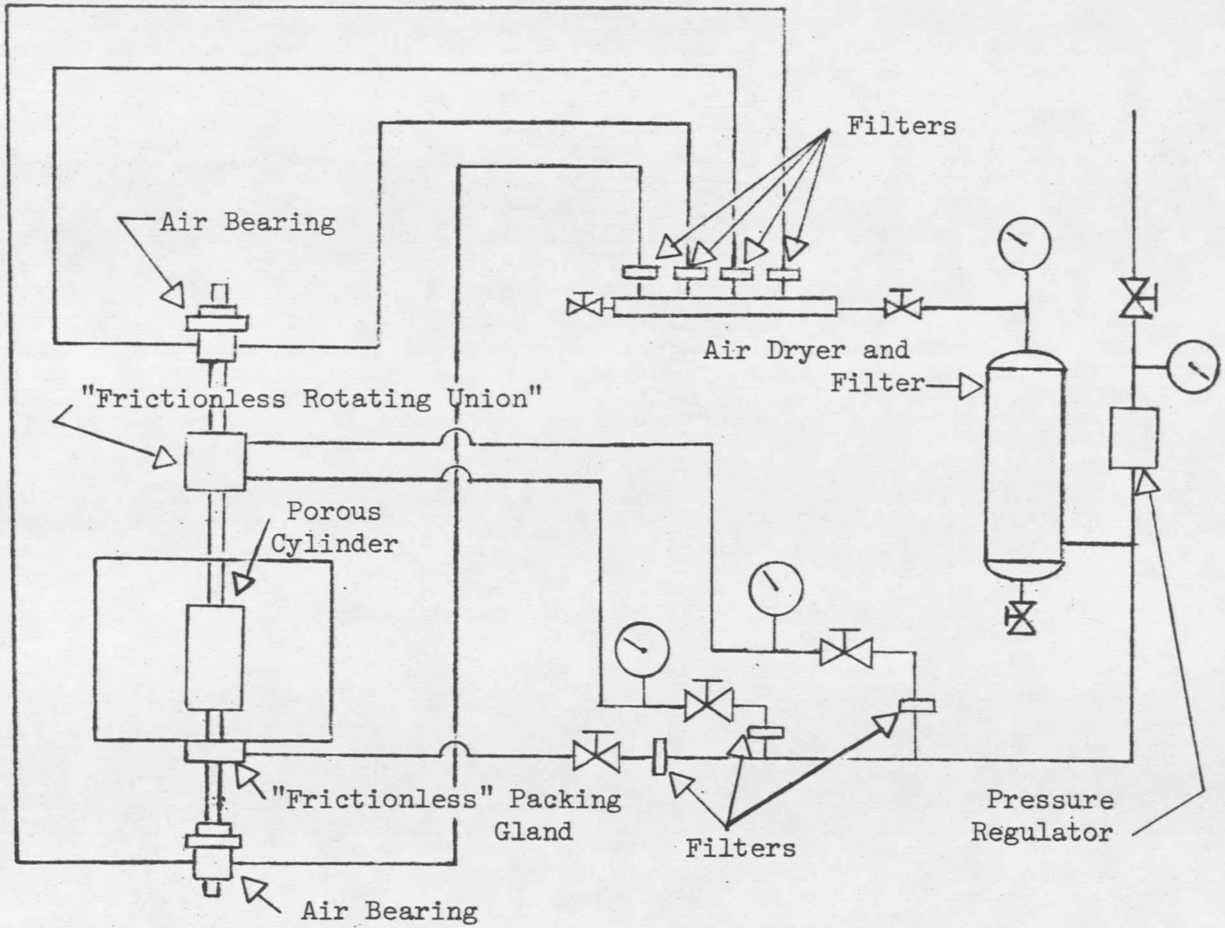

Figure 11. Air System for Moment Coefficient Experiment

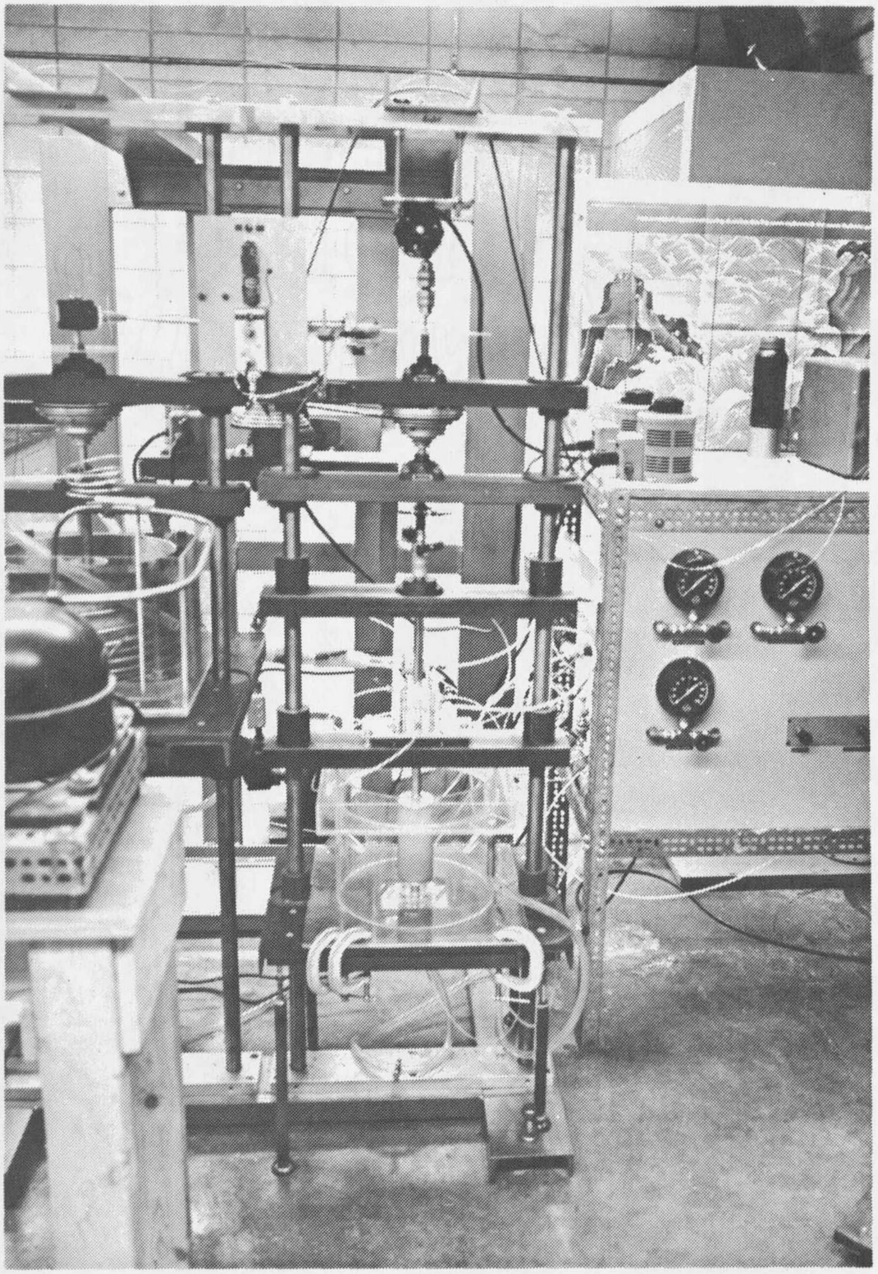

Figure 12. Moment Coefficient Equipment

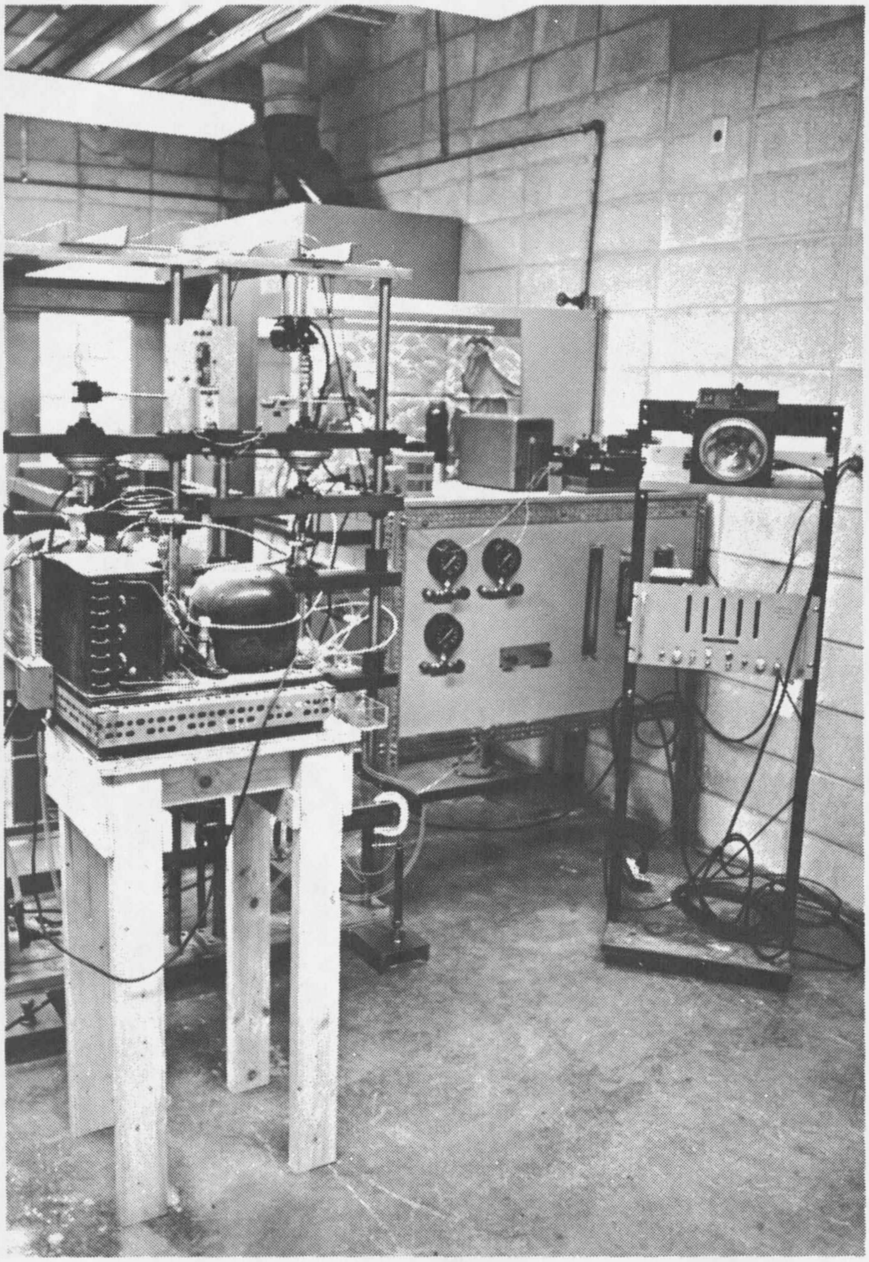

Figure 13. Equipment (Overall)

Figure 14. Equipment (Overall)

IV. RESULTS AND DISCUSSION

Several factors limited the range over which injection rate and angular velocity could be varied in the investigation. In the heat transfer experiment the largest flow rate used was 350 gm/min because of the low pressure available from the distilled water system. At very low flow rates and subsequent low heat transfer rates, the temperature difference across the tank became too small to measure accurately. Thus, the minimum flow rate varied from 20 gm/min at 76 RPM to 60 gm/min at 276 RPM. The lowest rotational speed available from the pulley system was 76 RPM. Other rotational speeds used were 102, 153, 205, and 276 RPM. At the next highest rotational speed--305 RPM--too much vibration resulted.

Injection rates in the moment coefficient experiment varied from 400 gm/min to 1600 gm/min at 60 RPM; below 400 gm/min no significant effect of injection could be detected. Sixteen hundred grams per minute was the maximum capacity of the pump. Injection was made only at 60 RPM since the lowest V_{θ_o}/V_{r_o} ratios were available at this speed. Below 60 RPM, the drive motor rapidly overheated because it had to be "lugged down" substantially to maintain constant speed. In determining moment coefficient without injection, the lowest rotational speed used was 30 RPM because the net torque became very small at this speed--0.6 gm-cm. The highest speed used was 363 RPM. Indeed, the eccentricity of the porous cylinders made torque readings above 200 RPM difficult because of oscillations.

Figures 15 and 16 are plots of Nusselt number versus Reynolds number and moment coefficient versus Reynolds number, respectively, for a rotating cylinder in a finite medium for the case of no mass transfer. There is no published data for the Nusselt number in the range of Reynolds numbers used in this experiment. However, Bilgen and Boulos (17) have published a significant amount of data for moment coefficient versus tip Reynolds number (Re_t). Comparison of Figure 17 and Table 1 shows excellent agreement. It is of interest, that while in this investigation the torque on the rotating cylinder was measured directly, Bilgen and Boulos, Taylor, and Donnelly determined the torque on the rotating cylinder by measuring the reaction on the outer cylinder; Theodorsen and Regier determined the torque on the rotating cylinder by measuring the energy required for rotation.

From Figure 16, it is clear that at a Reynolds number of 55,000 the slope of moment coefficient versus Reynolds number changes from positive to negative. Data of Schultz-Grunow and Hein in Schlichting (26) indicates transition flow at a Reynolds number of 7920 for small gap width. Furthermore, the range of tip Reynolds numbers used in this experiment is well within the turbulent flow regime defined by Bilgen and Boulos (17). It is beyond the scope of this investigation to speculate about the apparent flow transition at the Reynolds number of 55,000, and there is not enough data to warrant doing so. However, it is reasonable to suggest that transition Reynolds numbers may be very

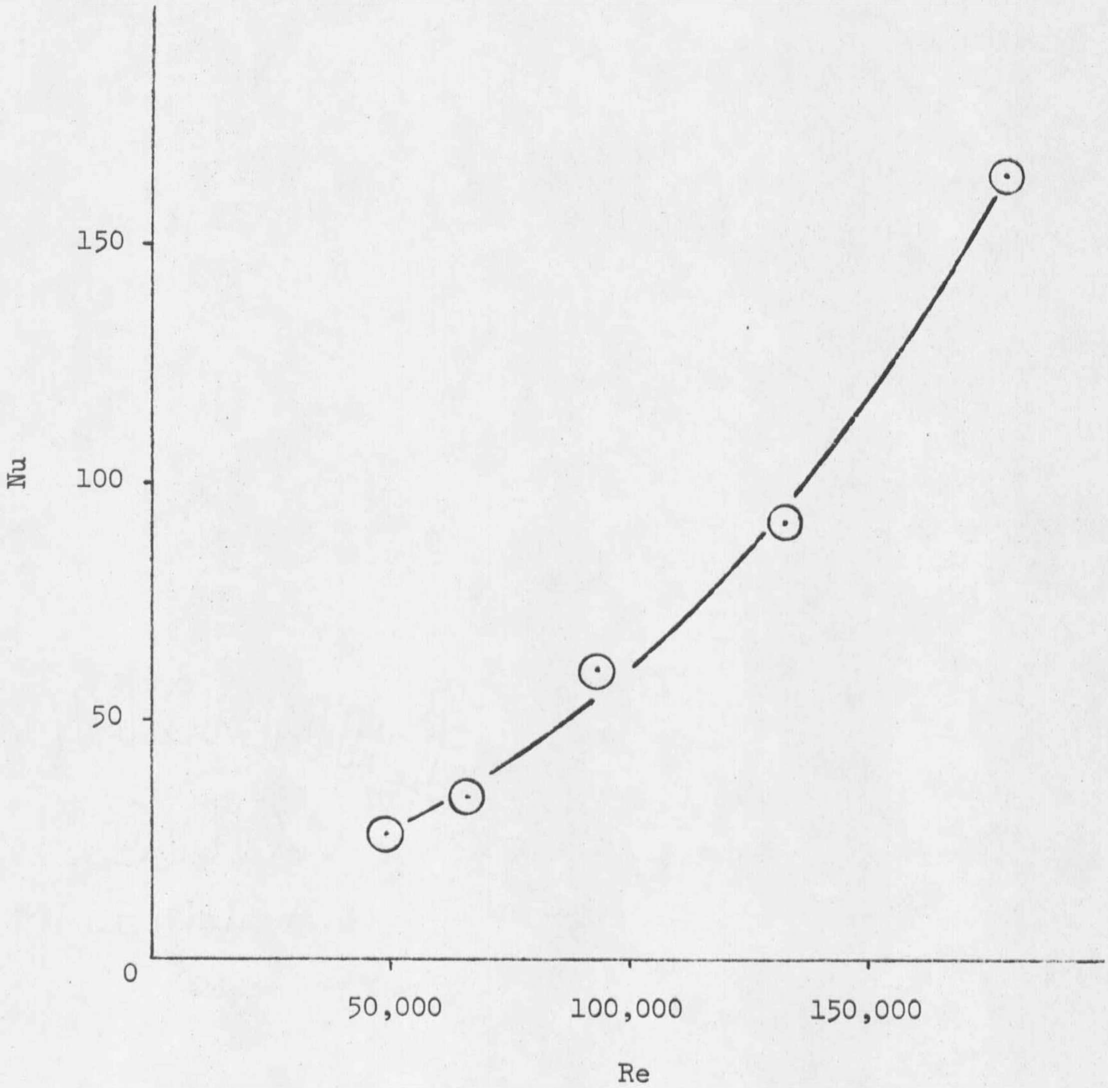

Figure 15. Nusselt Number versus Reynolds Number

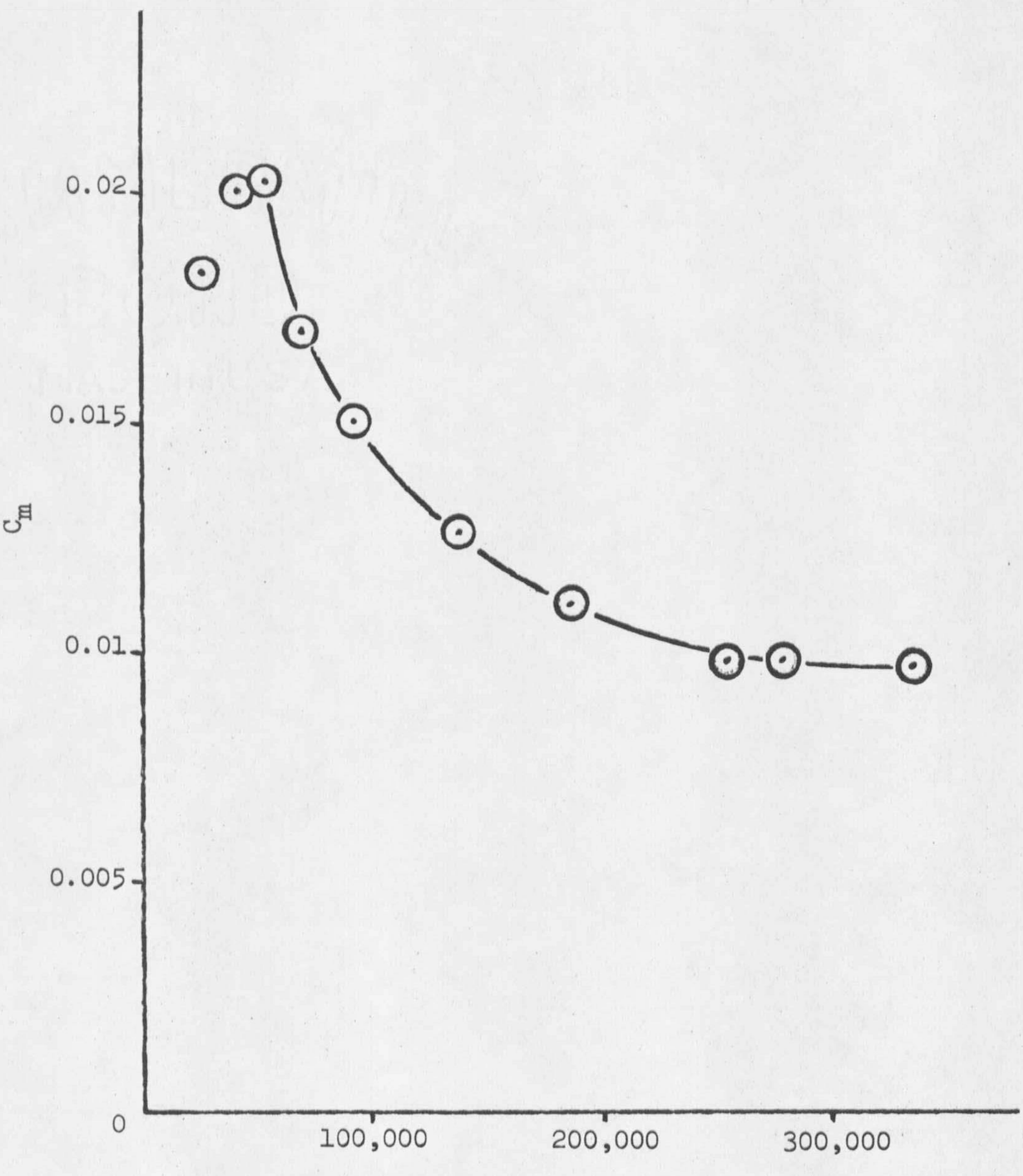

Figure 16. Moment Coefficient versus Reynolds Number

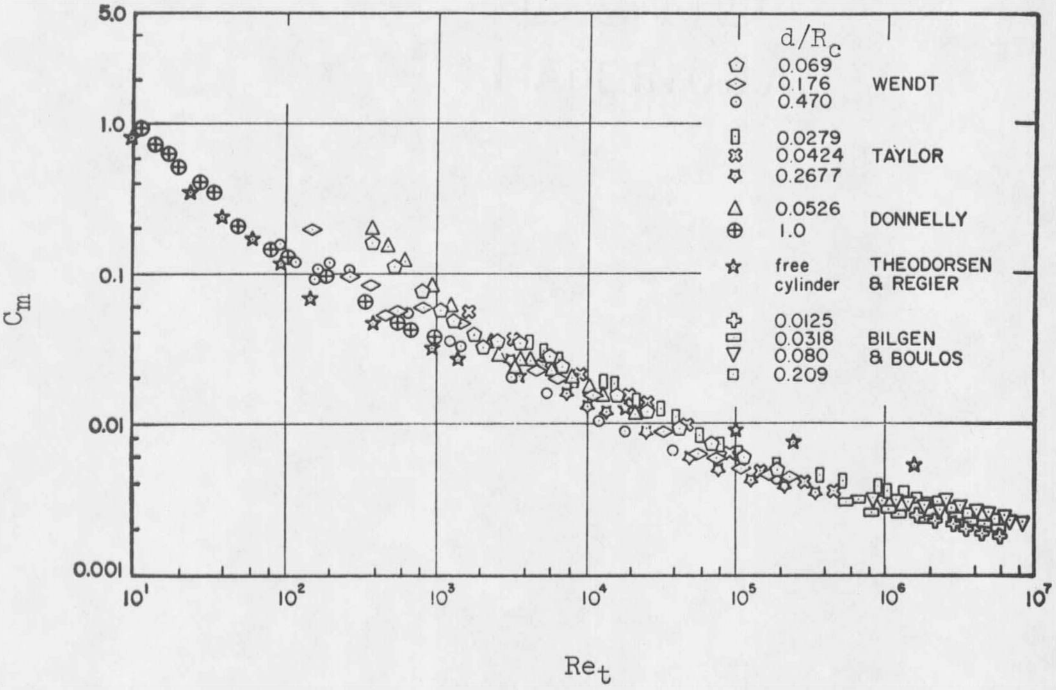

Figure 17. Moment Coefficient versus Tip Reynolds Number from Bilgen and Boulos (17)

Table 1. Moment Coefficient versus Tip Reynolds Number (Spannuth)

Re_t	C_m
3940	0.01825
6170	0.02005
7875	0.02025
9875	0.01702
13250	0.01506
20100	0.01267
26900	0.01109
37000	0.00985
40200	0.00991
47800	0.00975

different depending on gap width.

Figure 18 is a plot of the ratio of the heat transfer coefficient with mass transfer and the heat transfer coefficient without mass transfer versus the ratio of the angular and radial velocities at the cylinder surface. Figure 19 is a plot of the ratio of the moment coefficient with mass transfer and the moment coefficient without mass transfer versus the ratio of the angular and radial velocities at the cylinder surface. Clearly, the heat transfer and moment coefficients increase with mass transfer with the heat transfer coefficient increasing much more dramatically.

There is no published data for transpiration from a rotating cylinder. However, for the case of injection from flat plates and stationary cylinders in crossflow, experimental data shows the heat transfer coefficient decreasing with mass transfer for turbulent flow. Almost certainly, the anomaly can be explained by examination of the theory of the laminar sublayer. The hypothesis of a laminar sublayer for turbulent flow must be questioned for the case of a rotating cylindrical surface. The de-stabilizing effect of centrifugal force would be expected to result in secondary flows resembling Taylor vortices near the cylindrical surface. Such a phenomenon would not be conducive to the formation of a laminar sublayer. Therefore, it is hypothesized that no laminar sublayer exists on the surface of a rotating cylinder for turbulent flow. With transpiration, the assumption that no laminar

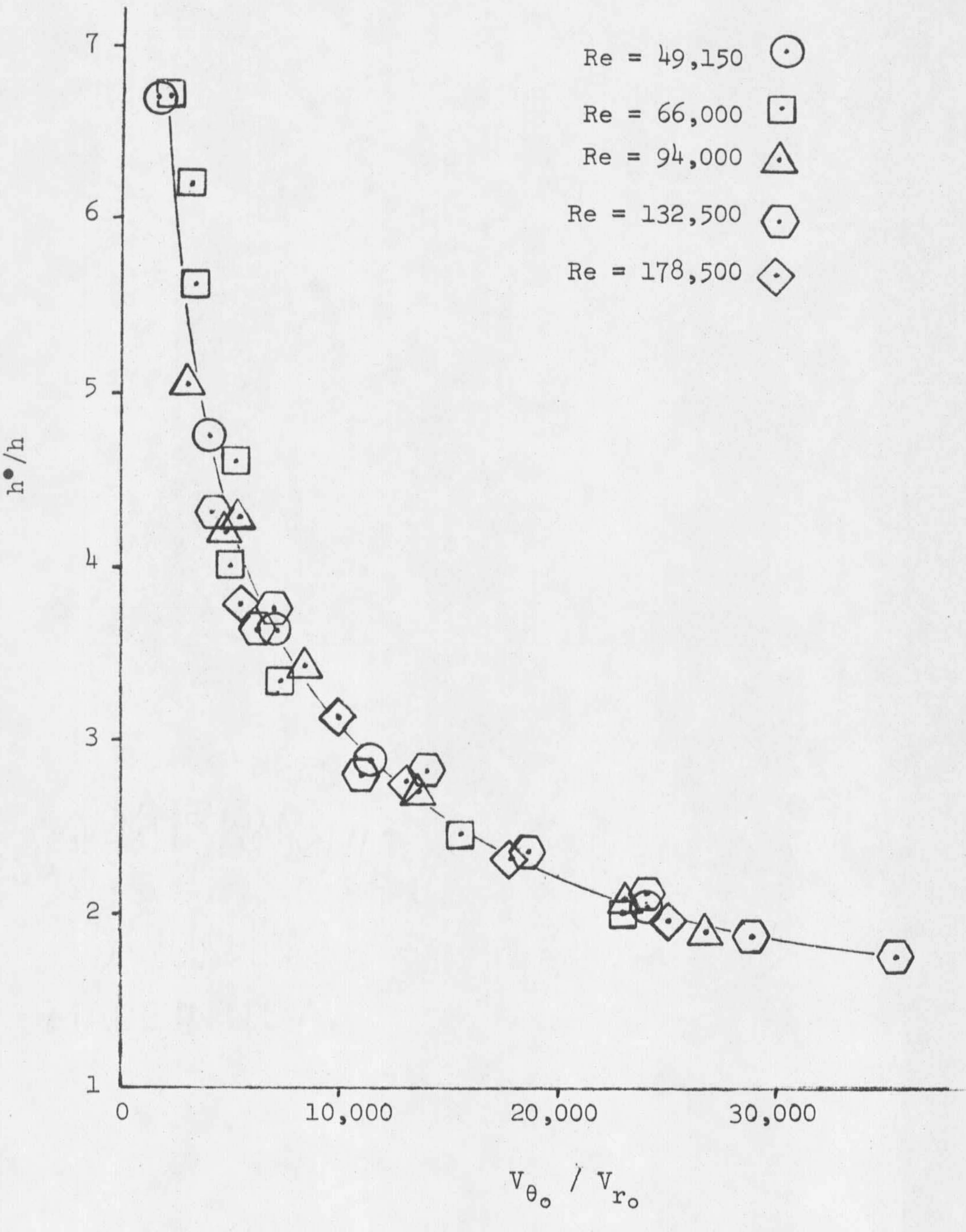

Figure 18. Heat Transfer Coefficient Ratio versus Velocity Ratio

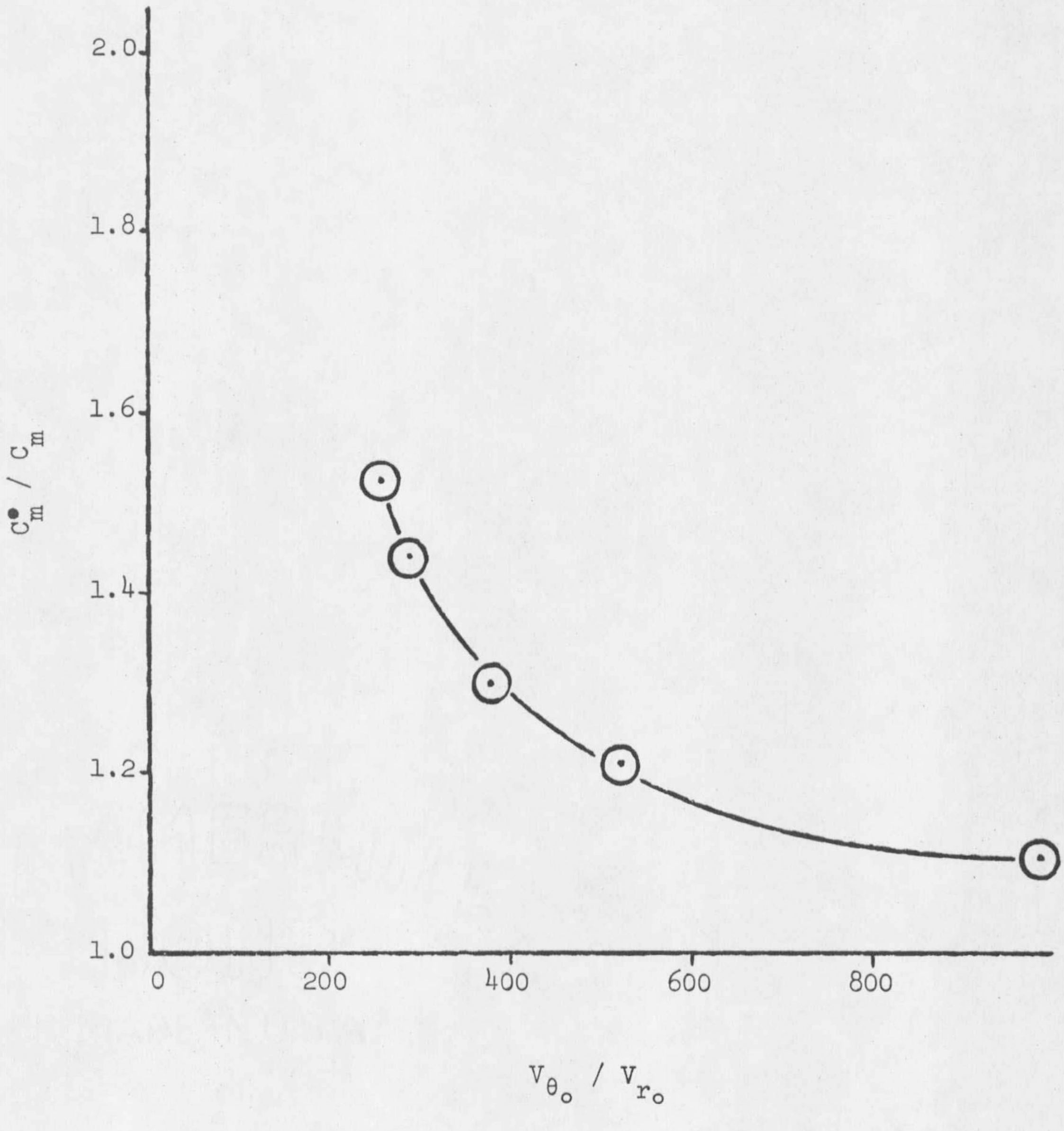

Figure 19. Moment Coefficient Ratio versus Velocity Ratio

sublayer exists can be more forcefully argued from experimental data. In order to discuss this assumption, equations for heat transfer and moment coefficients are presented.

Heat transfer for turbulent flow can be written as

$$q_o = \frac{mC_p}{A}(T_i - T_c) = h^\circ(T_c - T_t) = -k\left(1 + \frac{\varepsilon_H}{\alpha}\right)\frac{dT}{dr}\bigg|_{r = R_c} . \tag{9}$$

By substituting $R = r/R_c$ and $\Pi = (T - T_c)/(T_c - T_t)$, the equation for the heat transfer coefficient is

$$h^\circ = \frac{-k}{R_c}\left(1 + \frac{\varepsilon_H}{\alpha}\right)\frac{d\Pi}{dR}\bigg|_{R = 1} . \tag{10}$$

The force on the cylinder surface for turbulent flow with mass transfer is given by equation (11); the torque is given by equation (12):

$$F^\circ = \frac{2\pi R_c L V_{\theta_o} V_{r_o} \rho}{g_c} - \frac{2\pi R_c L \rho \upsilon}{g_c}\left(1 + \frac{\varepsilon_M}{\upsilon}\right)\left(\frac{1}{r}\frac{d\, rv_\theta}{dr}\right)\bigg|_{r = R_c} \tag{11}$$

and

$$\tau^\circ = \frac{2\pi R_c^2 L V_{\theta_o} V_{r_o} \rho}{g_c} - \frac{2\pi R_c^2 L \rho \upsilon}{g_c}\left(1 + \frac{\varepsilon_M}{\upsilon}\right)\left(\frac{1}{r}\frac{d\, rv_\theta}{dr}\right)\bigg|_{r = R_c} . \tag{12}$$

By substituting $R = r/R_c$ and $V_\theta = v_\theta/V_{\theta_o}$, equation (12) becomes

$$\tau^\circ = \frac{2\pi R_c^2 L V_{\theta_o} V_{r_o} \rho}{g_c} - \frac{2\pi R_c L V_{\theta_o} \rho \upsilon}{g_c}\left(1 + \frac{\varepsilon_M}{\upsilon}\right)\frac{d\, RV_\theta}{dR}\bigg|_{R = 1} . \tag{13}$$

By definition, $C_m = \tau g_c/0.5\pi\rho V_{\theta_o}^2 R_c^2 L$ so that

$$C_m^\circ = \frac{4V_{r_o}}{V_{\theta_o}} - \frac{8}{Re_\theta}\left(1 + \frac{\varepsilon_M}{\upsilon}\right)\frac{d\, RV_\theta}{dR}\bigg|_{R = 1} . \tag{14}$$

For the case of a laminar sublayer, the eddy viscosity--ε_M--and the eddy diffusivity of heat--ε_H--will be zero at the cylinder surface. Then from inspection of equation (10), the heat transfer coefficient would be proportional to the derivative $\frac{d\Pi}{dR}$, which is a negative quantity. It is easily argued that increasing mass transfer would result in the magnitude of $\frac{d\Pi}{dR}$ decreasing; hence, the heat transfer coefficient would decrease. Thus, the hypothesis of a laminar sublayer requiring the eddy diffusivity of heat to be zero at the cylinder surface is contrary to the experimental data.

This analysis is not applicable for the eddy viscosity, since from equation (14) the moment coefficient is the sum of two terms. However, it is unreasonable to expect the eddy viscosity to be zero at the cylinder surface when the eddy diffusivity of heat is not. To argue so is tantamount to proposing that a laminar sublayer existed in the moment coefficient experiment where one did not exist in the heat transfer coefficient experiment, even though the same cylinders, approximately the same gap widths, and the same range of Reynolds numbers were used.

It is reasonable to assume that the eddy viscosity and the eddy diffusivity of heat are different functions of the radius, the ratio of angular and radial velocities, the derivative $\frac{d\, rv_\theta}{dr}$, the Reynolds number, and the Prandtl number, i.e.,

$$\varepsilon_M = f_M\left(r, \frac{V_\theta}{V_r}, \frac{d\, rv_\theta}{dr}, Re\right) \tag{15}$$

and $\varepsilon_H = f_H(r, \frac{V_\theta}{V_r}, \frac{d\, rv_\theta}{dr}, Re, Pr).$ (16)

From Figures 18 and 19, h°/h is 2.0 at $V_{\theta_o}/V_{r_o} = 30{,}000$, whereas C_m°/C_m is only 1.5 at $V_{\theta_o}/V_{r_o} = 250$. Thus, the effect of the eddy diffusivity of heat on the heat transfer coefficient must be much more pronounced than the effect of the eddy viscosity on the moment coefficient. Undoubtedly, the magnitude of ε_H must be significantly larger than the magnitude of ε_M. Probably, ε_H is a much stronger function of V_θ/V_r than is ε_M, since for the case of no mass transfer, experimental data from Knudsen and Katz (27) shows that ε_H and ε_M are not greatly different for pipe flow, and, indeed, in the absence of data, it is often assumed that $\varepsilon_H = \varepsilon_M$.

In addition to experimental values for the heat transfer and moment coefficients, data on temperature and velocity profiles would also be required to determine eddy viscosities and eddy diffusivities of heat. Although it would be difficult to determine the functional relationships in equations (15) and (16), the problem is compounded because a single set of equations cannot describe the flow in the gap between concentric cylinders. Taylor (28) has shown that to account for experimental data on velocity profiles the Momentum Transport theory must be applied near surfaces, whereas the remainder of the flow where $\frac{d\, rv_\theta}{dr}$ is approximately zero must be described by the Vorticity Transport theory. Finally, the nature of the porous cylindrical surface would make an analysis of radial velocity extremely difficult. Perhaps, as is generally the case with turbulent flow, further investigation in transpiration from a rotating cylinder should be of an empirical, rather than a theoretical, nature.

V. CONCLUSIONS

From this investigation of transpirational heat and momentum transfer from a rotating cylinder the following conclusions were reached:

1. Heat transfer coefficients with no mass transfer increased with Reynolds number but were not comparable to published data,
2. Moment coefficients with no mass transfer decreased with Reynolds number and were in excellent agreement with published data except that
3. An apparent flow transition was observed at a Reynolds number of 55,000, and
4. With transpiration, heat transfer and moment coefficients increased with mass transfer with the heat transfer coefficient increasing much more dramatically.

Certainly, future investigations of transpiration from a rotating cylinder should involve different ratios of inside to outside cylinder radii and different Prandtl numbers so that the gap can be filled between published heat transfer coefficients with no mass transfer and those values in this report. Changes in these variables may also lead to a conclusion regarding the apparent flow transition found in the moment coefficient experiment. Probably, an attempt to determine eddy viscosities and eddy diffusivities of heat for the case of mass transfer would be extremely difficult so that an empirical, rather than a theoretical, approach would be more practical. With a sufficient amount of data, an analogy between heat and momentum transfer with (and without) mass transfer for a rotating cylinder in a finite medium with turbulent flow may be possible.

APPENDIX

Table 2. Nomenclature

Symbol	Explanation	Units
A	Area of cylinder	ft^2
C_m	Moment coefficient	dimensionless
C_m^o	Moment coefficient with mass transfer	dimensionless
C_p	Heat capacity	BTU/(lb)(°F)
d	Gap width, $R_t - R_c$	ft
F^o	Force on cylinder surface with mass transfer	lb force
F_{cw}	View factor	dimensionless
g_c	Constant, 32.17	$(lb)(ft)/(lb\ force)(sec^2)$
h	Heat transfer coefficient	$BTU/(hr)(ft^2)(°F)$
h^o	Heat transfer coefficient with mass transfer	$BTU/(hr)(ft^2)(°F)$
k	Thermal conductivity	BTU/(hr)(ft)(°F)
L	Cylinder length	ft
m	Mass flow rate	lb/hr
q	Rate of heat transfer	BTU/hr
q_o	Rate of heat transfer per unit area	$BTU/(hr)(ft^2)$
R, r	Radius	ft
R_c	Cylinder radius	ft
R_t	Tank radius	ft
T	Temperature	°F

Table 2. Nomenclature (continued)

Symbol	Explanation	Units
T_c	Temperature at cylinder surface	$^{\circ}F$
T_i	Temperature inside cylinder	$^{\circ}F$
T_{ref}	Reference temperature	$^{\circ}F$
T_t	Temperature at tank wall	$^{\circ}F$
V_θ, v_θ	Angular velocity	ft/sec
V_{θ_o}	Angular velocity at cylinder surface	ft/sec
V_r	Radial velocity	ft/sec
V_{r_o}	Radial velocity at cylinder surface; m/A	ft/sec
Nu	Nusselt number; hd/k	dimensionless
Pr	Prandtl number; $\upsilon/\alpha = C_p\mu/k$	dimensionless
Re	Reynolds number; $2dV_{\theta_o}/\upsilon$	dimensionless
Re_θ	Angular Reynolds number; $2R_cV_{\theta_o}/\upsilon$	dimensionless
Re_t	Tip Reynolds number; $\omega R_c^2/\upsilon$	dimensionless
σ	Stefan-Boltzmann constant	$BTU/(hr)(ft^2)(^{\circ}R^4)$
α	Thermal diffusivity; $k/\rho C_p$	ft^2/hr
ε	Emissivity	dimensionless
ε_H	Eddy diffusivity of heat	ft^2/hr
ε_M	Eddy viscosity	ft^2/hr
μ	Viscosity	lb/(ft)(sec)
υ	Kinematic viscosity	ft^2/hr
ω	Angular velocity	radians/sec

Table 2. Nomenclature (continued)

Symbol	Explanation	Units
ρ	Density	lb/ft^3
τ	Torque	(ft)(lb force)
τ^{o}	Torque with mass transfer	(ft)(lb force)
τ_o	Residual torque	(ft)(lb force)

Table 3. Experimental Data for Moment Coefficients

RPM	m (gm/min)	τ (gm-cm)	τ_o (gm-cm)
30	0	2.0	1.4
47	0	2.9	1.45
60	0	4.0	1.5
76	0	5.2	1.8
101	0	8.0	2.5
153	0	12.95	2.7
205	0	19.4	3.3
282	0	31.0	3.9
305	0	36.0	4.0
363	0	49.0	4.4
60	425	4.3	1.5
60	800	4.55	1.5
60	1100	4.85	1.5
60	1400	5.15	1.5
60	1600	5.35	1.5

Table 4. Experimental Data for Heat Transfer Coefficients

RPM	m (gm/min)	T_i (°F)	T_c (°F)	T_t (°F)
76	46.2	90	58.75	50.25
76	130.8	110	72.75	55.5
76	21.5	59	45	42.5
76	295.6	112.5	80	56
153	130.8	107.75	56.5	44.5
205	130.8	112.5	54	42.5
102	130.8	112	60.5	41.5
153	46.2	77	41.75	37
102	77.3	92.25	50.75	38.25
153	77.3	106	48	38.25
153	223	117.75	71.75	56.75
205	223	118.75	71.25	59
102	223	118.6	78	59
205	77.3	111.75	50	41.5
102	46.2	78	46	38.5
102	350	109	81.2	62
102	30	60.7	40.25	36.3
153	350	107.5	76	61.5
205	350	107.5	74.7	62
153	59.1	86	45.2	37.7
205	59.1	88.6	45.3	39.5
153	295.6	110	73.75	57.8
153	130.8	111.8	61.9	48.4
153	200	118.75	73.2	58.1
205	40	72.75	41.6	38.25
153	40	72.9	42.9	38.4
205	203.4	118.9	70	57.4
102	203.8	112.1	70.7	51.6
205	103	110.6	52.5	42.25
262	103	116	49.9	42.1
102	103	109.4	58	40.8
276	350	101.4	67.75	58.75
276	200	111.5	60	51.25
276	77	94.3	41.8	36.3
276	150	107	51.2	43.1
205	46.2	80.6	43.8	39.5
76	74	101.75	66	53.75

"FRICTIONLESS ROTATING UNION"

The principal design criteria for the "frictionless rotating union" was that there be no mechanical friction and negligible viscous friction in the device. These criteria were met by the device described in the Equipment section of the thesis. The concept of a device consisting of a chamber filled with injection fluid in which leakage through the gaps between the chamber and the rotating shaft was prevented by air pressure was rather easily translated into an operating piece of equipment.

Operation of the "frictionless rotating union" was considerably more difficult than design. At fluid pressures less than 20 psi, air entered the fluid chamber from the lower air chamber even with no air pressure on the lower air chamber. On the other hand, at 20 psi pressure on the fluid chamber, the required air pressures on the upper and lower air chambers for suitable operation were 40 psi and 2 psi, respectively. Clearly, operation of the device was more art than science and required considerable technique. Unequal tolerances between the chambers and the rotating shaft and the extremely complicated flow in the fluid chamber may have accounted for the wide range of pressures in the device. However, to obtain experimental data, it was only necessary to adjust air flow rates so that all the injection fluid entered the shaft; a technical explanation of flow phenomena was not required.

LIST OF REFERENCES

1. Rubesin, N.W., "An Analytical Estimation of the Effect of Transpiration Cooling on the Heat Transfer and Skin Friction Characteristics of a Compressible Turbulent Boundary Layer." NACA TN 3341, 1954.

2. Dorrance, W.H. and Dore, F.J., "The Effect of Mass Transfer on the Compressible Turbulent Boundary Layer Skin Friction and Heat Transfer," Journal of Aeronautical Sciences, Vol. 21 (1954), p. 404.

3. Mickley, H.A., et al., "Heat, Mass, and Momentum Transfer for Flow Over a Flat Plate with Blowing or Suction," NACA TN 3208, 1954.

4. Kays, William M., "Heat Transfer to the Transpired Turbulent Boundary Layer," Paper 71-HT-44 for ASME-AICHE Heat Transfer Conference Aug. 15-18, 1971.

5. Bird, R.B., Stewart, W.E., and Lightfoot, E.N., Transport Phenomena. (New York: John Wiley and Sons, Inc., 1960).

6. Elzy, E. and Wicks, C.E., "Transpirational Heat Transfer from a Cylinder in Cross Flow Including the Effects of Turbulent Intensity," Chemical Engineering Progress Symposium Series, Vol. 64 (1968), pp. 150-65.

7. Johnson, B.V. and Hartnett, J.P., "Heat Transfer from a Cylinder in Cross Flow with Transpiration Cooling," Journal of Heat Transfer, Vol. 85 (1963), pp. 173-79.

8. Cosart, William, Ph.D. Thesis Study at Oregon State University.

9. Erickson, L.E., et al., "Heat and Mass Transfer on a Moving Continuous Flat Plate with Suction or Injection," Ind. and Eng. Chem. Fundamentals, Vol. 5 (1966), p. 19.

10. Kirshan, B. and Rai, J., "Temperature Profile of a Fluid Between Two Rotating Porous Cylinders," Def. Sci. Journal, Vol. 20 (1970), pp. 183-86.

11. Mishra, S.P. ". . . .," Proc. National Inst. of India, Vol. 29 (1963), ...

12. Bahl, S.K., "Stability of Viscous Flow Between Two Concentric Rotating Porous Cylinders", Def. Sci. Journal, Vol. 20 (1970) pp. 89-96.

13. Gazley, Carl, Jr., "Heat Transfer Characteristics of the Rotational and Axial Flow between Concentric Cylinders," Trans. ASME, Vol. 80 (1958), pp. 79-90.

14. Becker, K.M. and Kaye, J., "Measurement of Diabatic Flow in an Annulus with an Inner Rotating Cylinder," Journal of Heat Transfer Vol. 84 (1962), pp. 97-105.

15. Bjorkland, I.S. and Kays, W.M., "Heat Transfer Between Concentric Rotating Cylinders," Journal of Heat Transfer, Vol. 81 (1959), pp. 175-86.

16. Sharman, R.D. et al., "Convective Heat Transfer Between Concentric Rotating Cylinders," AICHE Paper 1 for meeting Aug. 6-9, 1972.

17. Bilgen, E. and Boules, R., "Functional Dependence of Torque Coefficient of Coaxial Cylinders on Gap Width and Reynolds Numbers," Journal of Fluids Engineering, Vol. 95 Series I (1973), pp. 122-26.

18. Taylor, G.I., "Fluid Friction Between Rotating Cylinders, 1-Torque Measurements," Proceedings Royal Society, Series A, Vol. 157 (1936), pp. 546-64.

19. Wendt, F., "Turbulenete Stromungun Zwishen zwei rotierenden konaxiaten Zylindern," Ingenieur-Archiiv, Vol. 4 (1933), p. 401

20. Donnelly, R.J., "Experiments on the Stability of Viscous Flow Between Rotating Cylinders," Proceedings Royal Society, Series A, Vol. 246 (1958), p. 312.

21. Theodorsen, T. and Regier, A., "Experiments on Drag of Revolving Disks, Cylinders, and Streamline Rods at High Speeds," NACA Report No. 793, 1944.

22. Taylor, G.I., "Stability of a Viscous Liquid Contained Between Two Rotating Cylinders," Philosophical Transactions, Series A, Vol.223 (1923), p. 289.

23. Chandrasekhar, S., Hydrodynamic and Hydromagnetic Stability. (Oxford: Clarendon Press, 1961).

24. Chandrasekhar, S., "The Instability of a Layer of Fluid Heated Below and Subject to Cariolis Forces," Proceedings Royal Society, Series A, Vol. 217 (1953), pp. 306-27.

25. Dropkin, David and Globe, Samuel, "Effect of Spin on Natural Convection in Mercury Heated from Below," Journal of Applied Physics, Vol. 30 (1959), pp. 84-88.

26. Schlichting, H., Boundary-Layer Theory. (New York: McGraw-Hill Book Company, 1968).

27. Knudsen, J.G. and Katz, D.L., Fluid Dynamics and Heat Transfer. (New York: McGraw-Hill Book Company, 1958).

28. Taylor, G.I., "Distribution of Velocity and Temperature Between Concentric Rotating Cylinders," Proceedings Royal Society, Series A, Vol. 151 (1935), pp. 494-512.

Spannuth, Robert John
Transpirational heat and momentum transfer from a rotating cylinder

NAME AND ADDRESS